

Magnetic resonance spectroscopic imaging for detecting metabolic changes in glioblastoma after anti-angiogenic therapy—a systematic literature review

Mohamed E. El-Abtah[®], Pratik Talati, Jorg Dietrich, Elizabeth R. Gerstner, and Eva-Maria Ratai

Athinoula A. Martinos Center for Biomedical Imaging, Department of Radiology, Massachusetts General Hospital, Charlestown, Massachusetts, USA (M.E.E., P.T., E.M.R.); Department of Neurological Surgery, Massachusetts General Hospital, Boston, Massachusetts, USA (P.T.); Massachusetts General Hospital, Cancer Center, Boston, Massachusetts, USA (J.D., E.R.G.); Harvard Medical School, Boston, Massachusetts, USA (J.D., E.R.G., E.M.R.)

Corresponding Author: Eva-Maria Ratai, PhD, A.A. Martinos Center for Biomedical Imaging, Massachusetts General Hospital, 13th Street, Building 149, Room 2301, Charlestown, MA, 02129, USA (eratai@mgh.harvard.edu).

Abstract

Background. The impact of anti-angiogenic therapy (AAT) on patients with glioblastoma (GBM) is unclear due to a disconnect between radiographic findings and overall survivorship. MR spectroscopy (MRS) can provide clinically relevant information regarding tumor metabolism in response to AAT. This review explores the use of MRS to track metabolic changes in patients with GBM treated with AAT.

Methods. We conducted a systematic literature review in accordance with PRISMA guidelines to identify primary research articles that reported metabolic changes in GBMs treated with AAT. Collected variables included single or multi-voxel MRS acquisition parameters, metabolic markers, reported metabolic changes in response to AAT, and survivorship data.

Results. Thirty-five articles were retrieved in the initial query. After applying inclusion and exclusion criteria, 11 studies with 262 patients were included for qualitative synthesis with all studies performed using multi-voxel ¹H MRS. Two studies utilized ³¹P MRS. Post-AAT initiation, shorter-term survivors had increased choline (cellular proliferation marker), increased lactate (a hypoxia marker), and decreased levels of the short echo time (TE) marker, myo-inositol (an osmoregulator and gliosis marker). MRS detected metabolic changes as soon as 1-day after AAT, and throughout the course of AAT, to predict survival. There was substantial heterogeneity in the timing of scans, which ranged from 1-day to 6–9 months after AAT initiation.

Conclusions. Multi-voxel MRS at intermediate and short TE can serve as a robust prognosticator of outcomes of patients with GBM who are treated with AAT.

Key Points

- MR spectroscopy detects changes in tumor metabolism after anti-angiogenic therapy in GBM.
- MR spectroscopy predicts survival after anti-angiogenic therapy.
- Increase in choline and lactate as well as decrease in myo-inositol predicts early failure to AAT.

Glioblastoma (GBM) is the deadliest primary central nervous system tumor, and despite modest advancements in available treatment options, its prognosis remains dismal with a median survivorship of less than 24 months.¹ For several

decades, gadolinium-based contrast enhancement detected by T1-weighted magnetic resonance imaging (MRI) served as the best imaging marker for tumor detection and progression.² However, this has been complicated with the

Importance of the Study

Glioblastoma (GBM) carries a very dismal prognosis, with the median survivorship being less than 2 years. Although contrast-enhanced T1-weighted MRI has traditionally served as the imaging modality for detecting disease progression or response, the introduction of anti-angiogenic therapy (AAT) has made it necessary to integrate advanced MR modalities to detect tumor response. We conducted the first systematic literature review pertaining to the use of MR spectroscopy (MRS) to track metabolic

changes after AAT initiation in patients with GBM and how it predicts survival. Analysis of all studies showed that despite some heterogeneity in the MRS acquisition parameters and timing after AAT initiation, there was a consensus regarding common metabolic changes pertaining to markers of cellular proliferation, hypoxia, and osmoregulation. We emphasize the need for standardizing MRS protocols such that it can be routinely incorporated in clinical use.

advent of anti-angiogenic therapy (AAT) which can lead to a decrease in enhancement intensity without necessarily improving overall survival, a phenomenon known as pseudoresponse.^{3,4} Proposed mechanisms for this include changes in the permeability of the blood brain barrier (BBB) and a non-enhancing AAT-induced brain infiltration driven by vascular co-option.^{5,6} To that end, there has been much interest in the incorporation of other advanced MRI modalities to investigate markers that differentiate pseudoresponse from true response after initiating AAT.

¹H MR spectroscopy (MRS) can provide relevant information about the tumor microenvironment after initiation of AAT. In the healthy brain, the most prominent peak is derived from *N*-acetylaspartate (NAA) at 2.0 ppm. NAA is almost exclusively found in neurons and serves as a marker for neuronal integrity.⁷ Since most tumors are of non-neuronal origin, the NAA resonance is significantly reduced as neurons are replaced by neoplastic tissue.⁷ Other major peaks include creatine + phosphocreatine (Cr+PCr, commonly referred to as Cr) and choline (Cho), which are observed at 3.0 and 3.2 ppm, respectively. Notably, Cr is associated with neuronal bioenergetics and is in equilibrium with PCr, hence its peak remains stable in most disease states and is frequently used as an internal standard.⁸ Choline (Cho) is a marker for cellular proliferation and increased membrane turnover; it is directly correlated with tumor malignancy and a prominent Cho peak is a hallmark of many brain tumors.⁹ Lactate (Lac) is typically found in small concentrations (< 0.5 mM) in the brain and is mainly produced as a byproduct of anaerobic glycolysis, but can also be associated with necrosis.¹⁰ The doublet peak of Lac is observed at 1.32 ppm and is prominent in neoplastic tissue within the brain as cancer cells rewire their metabolism towards anaerobic glycolysis in a phenomenon known as the Warburg effect.^{9,11} In a previous prospective longitudinal clinical trial, it was shown that elevated Lac/NAA and decreased NAA/Cho in patients with recurrent GBM (rGBM) treated with AAT was associated with overall survival less than 9-months.¹²

MR spectra acquired with short echo times (TE) are characterized by resonances from myo-inositol (ml) at 3.5 ppm, glutamate + glutamine (Glx) at 2.3–2.4 ppm and 3.75 ppm, and lipids at 1.3 and 0.9 ppm. ml is an osmoregulator and glial marker that has been shown to be decreased in

more aggressive gliomas and in shorter-term survivors of GBM.^{6,13} Further, it is believed that disruptions to the BBB result in disturbances to osmotic equilibrium, resulting in lower ml concentrations.⁶ Although the resonance of glycine (Gly) overlaps with that of ml at short TE, it can be detected in isolation at longer TE due to the cancellation of the ml peak.¹⁴ Notably, high concentrations of Gly are observed in high-grade gliomas compared to lower-grade cancers.¹³ Lipids are found in necrotic tissue and serve as markers for high-grade malignancies.¹⁵

³¹P MRS can provide clinically relevant information on cellular bioenergetics. Specifically, it can measure adenosine triphosphate (ATP), phosphocreatine (PCr), phosphomonoester compounds such as phosphoethanolamine (PE) and phosphocholine (PC), and phosphodiester compounds such as glycerolphosphoethanolamine (GPE) and glycerolphosphocholine (GPC).¹⁶ Brain tumors show increased phosphomonoester/phosphodiester ratios compared to healthy brain tissue.^{17–19} Additionally, the chemical shift of the inorganic phosphate (Pi) is dependent upon the pH, and thus can be used to approximate *in vivo* intracellular pH.¹⁶ Increased extracellular acidosis within the tumor microenvironment causes an increase of intracellular pH.¹⁸

To measure MR spectra *in vivo*, one must be able to control the spatial origin of the detected signal. This can be done by using either single voxel spectroscopy (SVS) which incorporates selective excitation pulses to localize one voxel (2–8 cm³) at a time or by using 2D or 3D magnetic resonance spectroscopic imaging (MRSI), which results in multi-voxel arrays of spectra. SVS is appropriate for investigation of focal lesions, specific anatomical regions, or diffuse brain diseases as it is easier to execute. However, 2D or 3D MRSI is preferred when the location of interest is uncertain, multiple areas need to be simultaneously assessed, or there are heterogeneous metabolite distributions across a lesion, which is the case with GBM.²⁰

Another important consideration for ¹H MRS is the acquisition scheme which includes Point Resolved Spectroscopy (PRESS), Stimulated Echo Acquisition Mode (STEAM), localization by adiabatic selective refocusing (LASER), or semi-LASER (sLASER) pulse sequences. While STEAM allows for shorter minimum TE and results in better localization performance over PRESS, it only uses 50% of the

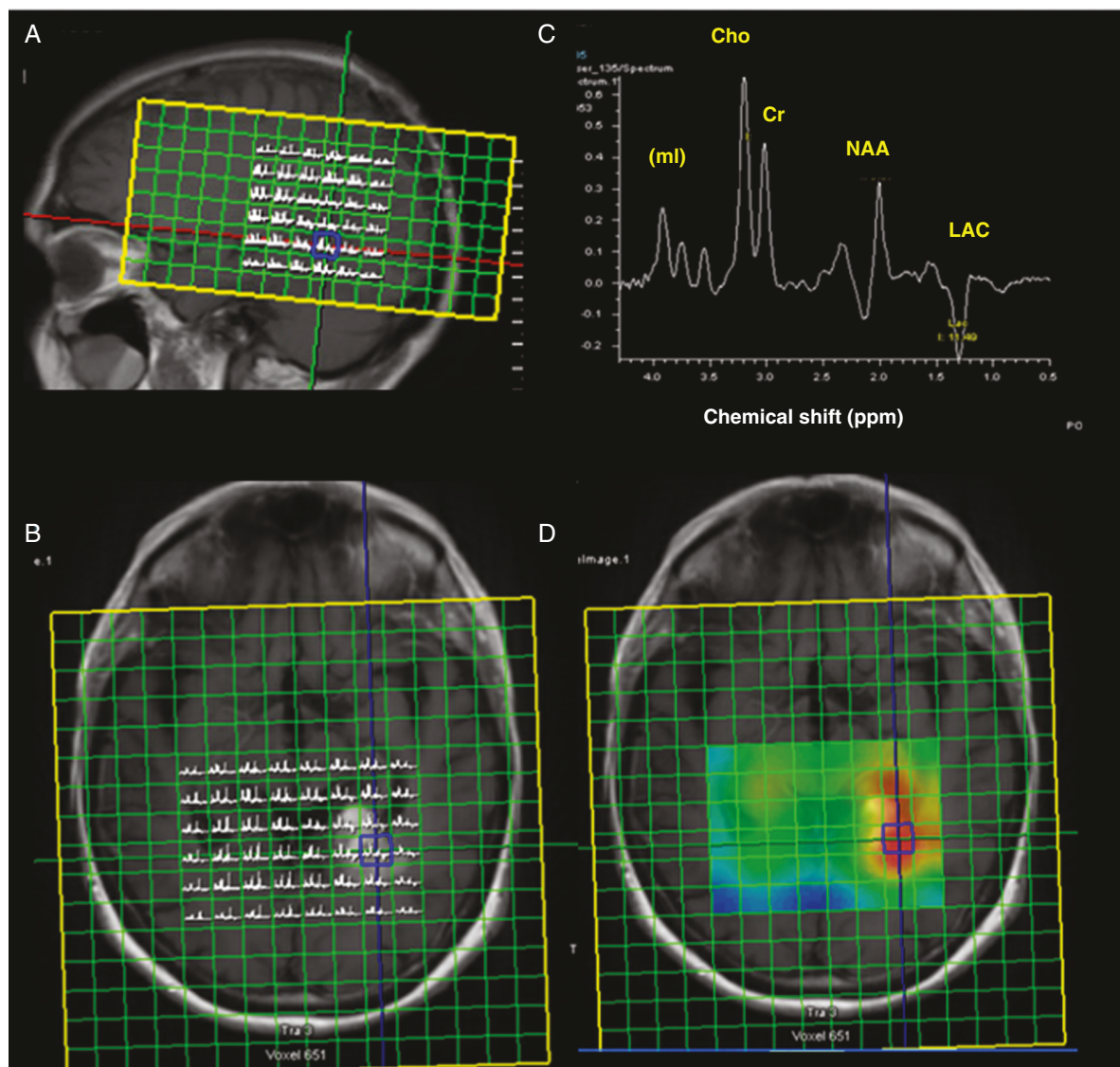


Figure 1. Representative multi-voxel MRS acquisition of a brain tumor. Sagittal (A) and axial (B) views of a patient with a brain tumor with a multi-voxel MRS grid overlaid are shown. The intermediate TE spectra from a representative voxel highlighted in blue is displayed in (C). Since this spectrum was obtained at intermediate TE, ml would not be detectable although its relative position is denoted by the parentheses. A metabolic map highlighting Choline levels shows a “hot spot” at the location of the GBM (D).

available signal. On the other hand, sLASER and LASER provide sharper slice selection profiles, minimize chemical shift displacement errors, and improve localization, spectral quality, and repeatability.^{20,21} Figure 1 is a representative 3.0 T multi-voxel MRS acquisition of a brain tumor using sLASER acquisition scheme at TE = 135 ms. For ³¹P data acquisition, typical acquisition schemes include free induction decay (FID) which results in no localization except for coil penetration, image-selected in vivo spectroscopy (ISIS) for single voxel acquisition, and 2D chemical shift imaging (CSI) from a matrix of voxels.

Despite numerous reports on the incorporation of MRSI to investigate metabolic changes after AAT in patients with GBM,^{6,12,22} there remains uncertainty regarding which MRS

methodology to use, and how and when to incorporate MRS within the clinical management of patients. This is partly due to heterogeneity in the timing of MRSI acquisition post-AAT initiation, need for technical expertise to methodologic ally implement MRSI, and the lack of consensus on metabolites of interest. The aim of this review is to assess the current state of how MRSI is clinically used to track metabolic changes in patients with GBM who are treated with AAT. An understanding of the various acquisition schemes, acquisition parameters, metabolic markers, and their associated prognostic values may help clinicians understand how AAT impacts tumor biology, distinguish between pseudo response and treatment response early in the disease course, identify patients early on who

benefit the most from AAT, and optimize the timing of MRS throughout the course of clinical management.

Methods

Systematic Review

This study was a systematic literature review performed according to the Preferred Reporting Items for Systematic Review and Meta-Analyses (PRISMA) 2009 guidelines.²³ A structured literature search was performed to capture all clinical studies published in English involving the use of single or multi-voxel MRS to detect metabolic changes in patients with GBM, including those with known recurrence treated with AAT. The search queried PubMed using the following terms: (“magnetic resonance spectroscopy”[MeSH Terms] OR “spectroscopic”[All Fields] OR (“magnetic”[All Fields] AND “resonance”[All Fields] AND “spectroscopy”[All Fields]) OR “magnetic resonance spectroscopy”[All Fields] OR (“mr”[All Fields] AND “spectroscopy”[All Fields]) OR “mr spectroscopy”[All Fields] OR “MRS”[All Fields]) AND (“angiogenesis inhibitors”[Pharmacological Action] OR “angiogenesis inhibitors”[MeSH Terms] OR (“angiogenesis”[All Fields] AND “inhibitors”[All Fields] OR “angiogenesis inhibitors”[All Fields] OR “bevacizumab”[All Fields] OR “cediranib”[All Fields] OR “antiangiogenic”[All Fields] OR “antiangiogenic”[All Fields] OR “antiangiogenics”[All Fields]) AND (“glioblastoma”[MeSH Terms] OR “glioblastoma”[All Fields] OR “glioblastomas”[All Fields] OR “GBM”[All Fields]).

Thirty-five articles were retrieved in the initial PubMed query. Two authors (MEE, EMR) completed the title and abstract screening, based on inclusion and exclusion criteria that were determined a priori. Notably, both authors were blinded to each other’s results and any disagreements were adjudicated by a third author (PT). The exclusion criteria were: 1) articles not published in English, 2) review articles, case reports, or any non-peer-reviewed articles, and 3) animal studies. Inclusion criteria were defined as follows: 1) reporting of MRS acquisition parameters, 2) quantitative analysis of metabolic markers, 3) inclusion of survivorship and/or clinical outcomes measures, and 4) diagnosis of GBM or recurrent GBM. Following the application of the aforementioned criteria, 24 studies were included for full-text screening. Inclusion and exclusion criteria for full-text review were applied by two reviewers, who were blinded to each other’s results.

Data Extraction and Management

We utilized a systematic data extraction checklist to code important study characteristics such as author, year, study design, demographics, single or multi-voxel MRS acquisition parameters, acquisition schemes, metabolic markers, survivorship, and clinical outcomes. Additionally, we used a modified version of the Methodological Quality Rating Scale (MQRS) to rate the methodological quality of all the incorporated studies.²⁴ Based on dimensions such as study

design and replicability, the cumulative MQRS score may range from 1 (poor quality) to 16 (high quality).

Results

Data Extraction

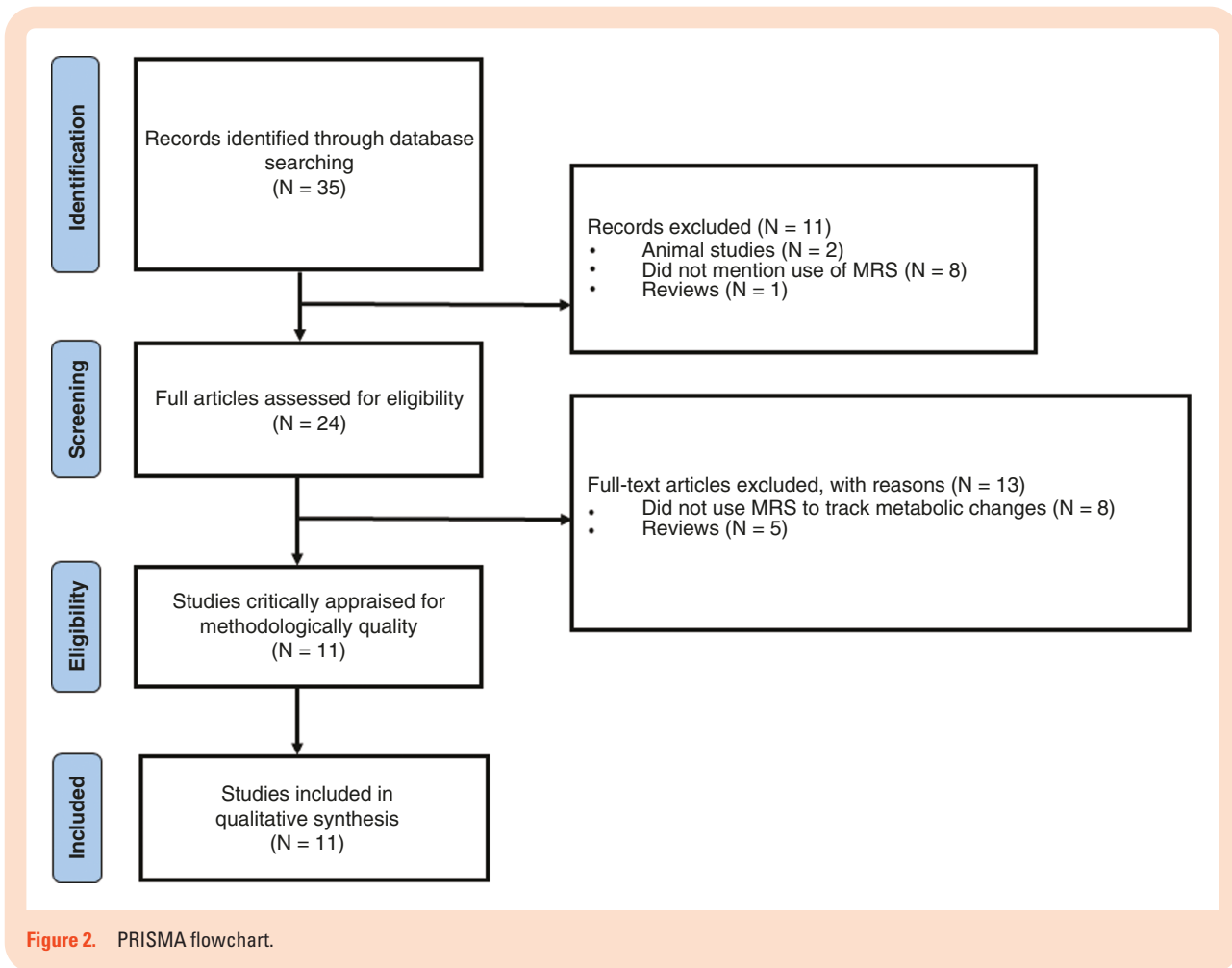
After completing a full-text review, 11 studies were included for qualitative synthesis as summarized in the PRISMA flowchart (Figure 2). Detailed study characteristics, including demographics, treatments, main findings, and MQRS score are highlighted in Table 1. Ten of the 11 studies (10/11; 91%) were prospective, one study was a Phase I/II clinical trial, and all studies were published between 2011 and 2022. In total, we extracted data from a total of 262 patients and gender was reported for 210 patients (135/210 men; 64.3%). The largest study was by Talati et al.,¹² which reported data from 33 patients at baseline (prior to AAT initiation), and up to 25 patients during the course of AAT. The median MQRS score was 12 (range: 10–14). All studies incorporated the use of multi-voxel MRSI as the main imaging modality for tracking metabolic changes in patients with confirmed GBM.

Treatment Regimens

A total of ten studies were performed on patients with recurrent GBM^{6,12,17,22,25,27,28,29,30,31} (10/11; 90.9%) and 1 study was performed on patients with newly diagnosed GBM²⁶ (1/11; 9.1%). All patients underwent surgical resection or biopsy followed by chemoradiation. Exact treatment regimens were reported for 262 patients. Bevacizumab, an anti-VEGF monoclonal antibody, was used in the treatment regimens of 210 patients (210/262; 80.2%) and cediranib, an oral pan-VEGF receptor tyrosine kinase inhibitor, was used in the treatment regimens of 52 patients (52/262; 19.8%). One hundred thirty-four patients received AAT as monotherapy (134/262; 51.1%), 123 patients received combination therapy which included AAT (123/262; 46.9%), and 5 patients received concomitant radiotherapy (RT) and AAT (5/262; 1.9%). Of the 123 patients who received combination therapy, 25 received AAT and temozolomide (TMZ) (25/262; 9.5%), 2 received AAT and an immune checkpoint inhibitor (2/262; 0.8%), 24 received AAT and lomustine (24/262; 9.2%), 19 received AAT and irinotecan (19/262; 7.3%), 31 received RT, AAT, TMZ, and erlotinib (31/262; 11.8%), 1 received AAT and topotecan (1/262; 0.4%), and 21 received AAT, RT, and TMZ (21/262; 8.0%). Bevacizumab was intravenously injected in all patients except those reported by Jeon et al.²⁵ where it was delivered via intra-arterial cerebral infusion to overcome toxicity, impedance of the BBB, and enhance delivery. A summary of all the treatment regimens reported by the studies is included in Table 1.

MRSI Acquisition Parameters

All studies utilized multi-voxel MRS, with no studies reporting the use of single voxel MRS. We extracted the following MRSI parameters: nuclear magnetic resonance



(NMR) nucleus, acquisition scheme, magnetic field strength of MRI scanners, TE, and repetition time (TR). All of the included studies performed ^1H MRS^{6,12,17,22,25,26,27,28,29,30,31} and the most frequently used acquisition scheme was PRESS (9/11; 81.8%), followed by LASER (3/11; 27.3%), and section-interleaved spin-echo sequence³² (1/11; 9.1%). Two studies performed ^{31}P MRS and used CSI-FID as the acquisition scheme (2/11; 18.2%). Notably, the studies by Talati et al. and El-Abtah et al. both used LASER and PRESS acquisition schemes,^{6,12} while the study by Wenger et al.²⁹ used both PRESS and CSI-FID. All of the studies incorporated ^1H MRSI with 5 studies incorporating short TE (30–45 ms), 6 studies incorporating intermediate TE (135–144 ms), and 1 study incorporating long TE (> 270 ms). El-Abtah et al.⁶ reported using multi-echo spectroscopy (short and intermediate TE) for the acquisition of metabolic ratios. There was heterogeneity regarding TR used, which ranged from 1104 to 2300 ms, and 4 studies (4/11; 36.4%) utilized two different TRs.^{6,12,26,27} We also observed heterogeneity regarding the MRSI voxel resolutions reported, which ranged from 1 to 2.7 cm³. Since ^{31}P MRSI is substantially different than ^1H MRSI, we analyzed those acquisition parameters separately. Hattingen et al. and Wenger et al. incorporated ^{31}P MRSI (free induction decay) as a supplemental modality with a TE of 2.3 ms, a TR of 2000 msec, and a voxel

resolution of 22.5 cm³.^{17,29} A summary of all the MRSI acquisition parameters is included in Table 2.

The criteria used for ensuring quality control of the spectra varied across the studies. For example, the study by Andronesi et al.³¹ only included voxels for which the goodness of fit as measured by Cramer-Rao lower bounds were less than 20%, while the study by Kim et al.³⁰ used a full width at half maximum (FWHM) below 20Hz for the water signal. Furthermore, other studies incorporated a quality control measure which consisted of visual inspection for artifacts according to the criteria described by Kreis et al.³³

MR Spectroscopic Markers of Cellular Proliferation

Seven studies (7/11; 63.6%) discussed metabolic changes associated with malignancy, cellular proliferation, and membrane turnover (Table 3).^{12,17,22,25,27,30,31} Jeon et al.²⁵ assessed the anti-proliferative effects of AAT, as measured by the ratio of total Cho to NAA (tCho/NAA). After super-selective intra-arterial cerebral infusion of AAT, there was a significant decrease of 26% in tCho/NAA relative to pre-treatment levels within regions of enhancing disease. Of

Table 1. Summary of study characteristics

Author, year	Study design	Study setting	Population	Treatment regimen details	Main findings/conclusion	MORS score
El-Abtah, 2022 ⁶	Prospective, Longitudinal Study	Single-center, United States	N = 21 Mean age: 62 Male (%): 71	Bevacizumab monotherapy: 5 Bevacizumab + TMZ: 5 Bevacizumab + Anti-PD-1: 1 Bevacizumab + Lomustine: 10	Lower levels of ml normalized by contralateral creatine in the intratumoral, peritumoral, and contralateral volumes are predictive of poor survivorship and anti-angiogenic treatment failure	12
Hattingen, 2013 ¹⁷	Prospective Registry Study	Single-center, Germany	N = 32 Median age: 53 Male (%): 66	Bevacizumab: 23 Bevacizumab + Irinotecan: 9	Elevated PCho/GPC ratio is predictive of shorter-OS	11
Jeon, 2012 ²⁵	Phase I/II Clinical Trial	Single-center, United States	N = 18 Mean age: 48 Male (%): 61	Superselective intra-arterial cerebral infusion of Bevacizumab: 18	Treatment of rGBM with SIACI anti-angiogenic therapy is associated with significant reductions in tCho/NAA in enhancing regions after intervention	12
Nelson, 2016 ²⁶	Prospective Study	Single-center, United States	N = 31 Median age: 52 Male (%): 48%	Bevacizumab + RT + TMZ + erlotinib: 31	There were significant reductions in Choline/NAA and Cho/Cr after treatment initiation, with changes in levels of lactate and lipids suggestive of vascular normalization	13
Ratai, 2013 ²⁷	Prospective Study	Multi-center, United States, Israel	N = 13 Mean age: 55 Male (%): 69%	Bevacizumab + TMZ: 9 Bevacizumab + irinotecan: 4	NAA/Cho levels increased and Cho/Cr levels decreased within the enhancing tumor at 2 weeks after BL, suggesting an antitumor effect of anti-angiogenic therapy in combination with cytotoxic chemotherapy	12
Steidl, 2016 ²⁸	Prospective Study	Single-center, Germany	N = 30 Median age: 52 Male (%): 73%	Bevacizumab monotherapy: 18 Bevacizumab + irinotecan: 6 Bevacizumab + topotecan: 1 Bevacizumab + RT: 5	ml levels significantly increased during anti-angiogenic therapy, with higher ml concentrations at BL and higher differences between control and tumoral volumes suggestive of longer survival	12
Talati, 2021 ¹²	Prospective, Longitudinal Study	Single-center, United States	N = 33 Median age: 63 Male (%): 70	Bevacizumab monotherapy: 7 Bevacizumab + TMZ: 11 Bevacizumab + Anti-PD-1: 1 Bevacizumab + Lomustine: 14	Changes in metabolic ratio of tumoral NAA/Cho and Lac/NAA are early biomarkers for predicting survivorship and response to anti-angiogenic therapy. Elevated NAA/Cho and decreased Lac/NAA were markers of responses to anti-angiogenic therapy	13
Wenger, 2017 ²⁹	Prospective, Longitudinal Study	Single-center, Germany	N = 14 Median age: 51 Male (%): 79	Bevacizumab monotherapy: 14	Elevated intracellular pH as detected by ¹ H/ ³¹ P MRSI in unaffected tissue at baseline precedes MRI-detectable GBM progression in patients treated with anti-angiogenic therapy	10
Stadlbauer, 2015 ²²	Prospective, Longitudinal Study	Single-center, Germany	N = 18 Mean age: 53.1 Male (%): 56	Bevacizumab monotherapy: 18	Cho and NAA concentrations and Cho/NAA can distinguish between responders and non-responders of anti-angiogenic therapy, particularly at 6–9 months after therapy initiation	12
Kim, 2011 ³⁰	Prospective, Longitudinal Study	Single-center, United States	N = 31 Mean age: 53.7 Male (%): NR	Cedarinib monotherapy: 31	Enhancing tumor NAA/Cho is predictive of 6-month overall survivorship. Notably, enhancing tumor NAA/Cho was unchanged through day 28, increased from day 28–56, and subsequently decreased, consistent with clinical course of recurrence	12
Andronesi, 2017 ³¹	Prospective, Longitudinal Study	Single-center, United States	N = 21 Mean age: NR Male (%): NR	Cedarinib + RT + TMZ	The ratio of tCho/c-Cr after 1 month of treatment was significantly associated with overall survivorship, based on area under the curve analyses	14

TMZ, temozolomide; RT, radiotherapy; ml, myo-inositol; PCho/GPC, ratio of phosphocholine to glycerophosphocholine; OS, overall survivorship; NAA/Cho, ratio of *N*-acetylaspartate to choline; Cho/Cr, ratio of choline to creatine; Lac/NAA, ratio of lactate to *N*-acetylaspartate; tCho/NAA, ratio of total choline to NAA; tCho/c-Cr, ratio of total choline to creatine in contralateral normal appearing white matter tissue.

Table 2. MRSI acquisition parameters

Author, year	Magnetic field strength of MRI scanners	NMR nucleus	Acquisition scheme	Echo-time (TE) in ms	Repetition time (TR) in ms	MRSI voxel resolution in cm ³
El-Abtah, 2022 ⁶	1.5T and 3T	¹ H	3D MRSI 2D MRSI	30 and 135	1500 or 1700	1 or 1.44
Hattngen, 2013 ^{17,*}	3T	¹ H	3D MRSI	30	1500	2.25
Hattngen, 2013 ^{17,*}	3T	³¹ P	3D MRSI	2.3	2000	22.5
Jeon, 2012 ²⁵	3T	¹ H	Multi-section 2D MRSI	280	2300	2.16
Nelson, 2016 ²⁶	3T	¹ H	3D MRSI	144	1104 or 1300	1
Ratai, 2013 ²⁷	1.5T and 3T	¹ H	2D MRSI	144	1500 or 1700	3.4 or 1 or 1.5
Steidl, 2016 ²⁸	3T	¹ H	3D MRSI	30	1500	2.25
Talati, 2021 ¹²	1.5T and 3T	¹ H	3D MRSI 2D MRSI	135	1500 or 1700	1 or 1.44
Wenger, 2017 ^{29,*}	3T	¹ H	3D MRSI	30	1500	2.7
Wenger, 2017 ^{29,*}	3T	³¹ P	3D MRSI	2.3	2000	22.5
Stadlbauer, 2015 ²²	3T	¹ H	3D MRSI	135	1600	1
Kim, 2011 ³⁰	3T	¹ H	2D MRSI	135 or 144	1700	1.4
Andronesi, 2017 ³¹	3T	¹ H	3D MRSI	45	1500	1.5 or 4.8

*These studies incorporated the use of ³¹P and ¹H MRSI with varying acquisition parameters. LASER, localized by adiabatic selective refocusing; PRESS, Point RESolved Spectroscopy; CSI, chemical shift imaging; FID, free induction decay.

Table 3. Summary of MRS studies

Author, year	Metabolic marker	Changes in metabolic markers observed with AAT
Summary of studies reporting MRS markers related to cellular proliferation		
Hattingen, 2013 ¹⁷	PCho/GPC	Patients with shorter-OS had elevated intratumoral PCho/GPC relative to the contralateral normal appearing tissue before AAT initiation. PCho/GP significantly decreased 8-weeks after AAT initiation and subsequently increased at the time of progression
Jeon, 2012 ²⁵	tCho/NAA	tCho/NAA significantly decreased when measured 3–5 weeks after AAT initiation
Kim, 2011 ³⁰	NAA/Cho; NAA/c-Cr; Cho/c-Cr	Intratumoral NAA/Cho was unchanged from baseline until 28 days after AAT initiation. NAA/Cho significantly increased through 56 days post treatment, followed by a significant decrease at the time of progression
Ratai, 2013 ²⁷	NAA/cr; NAA/Cho; Cho/cr	Decreased peritumoral Cho/cr and increased NAA/cr and NAA/Cho at 16 weeks after AAT were predictive of PF-6 and OS at 1 year
Talati, 2021 ¹²	NAA/Cho	Increased NAA/Cho from baseline was predictive of OS at 9 months at 1 day, 2 weeks, 8 weeks, and 16 weeks after AAT initiation
Stadlbauer, 2015 ²²	NAA/cr; NAA; Cho/NAA	Responders to AAT had a significant decrease in Cho and Cho/NAA from baseline to 234 days after AAT initiation. The opposite trend was noted in non-responders
Andronesi, 2017 ³¹	tCho/NAA; tCho/c-Cr	Longer-term survivors, with OS > 18.2 months, had significant reductions in tCho/c-Cr at 15 and 29 days after initiating cediranib and chemoradiation. Shorter-term survivors showed greater stability in levels of tCho/c-Cr throughout the 6-weeks of longitudinal follow-up
Summary of studies reporting MRS markers related to hypoxia		
Talati, 2021 ¹²	Lac/NAA	Shorter-term survivors exhibited increased Lac/NAA relative to the pre-AAT baseline
Wenger, 2017 ²⁹	pH	Elevated intracellular pH precedes radiographic progression of GBM
Nelson, 2016 ²⁶	Lac and lipids	Lactate and lipids significantly decreased at 2 weeks after RT completion and 4 months after AAT and RT initiation
Jeon, 2012 ²⁵	Lac	There was a modest decrease in the Lac peak within a single voxel in the corpus callosum after AAT
Summary of studies reporting MRS markers related to osmoregulation and gliosis		
Steidl, 2016 ²⁸	ml	After AAT initiation, ml was significantly increased in the intratumoral and contralateral normal appearing tissue. Longer-term survivors exhibited greater difference in ml between intratumoral and contralateral normal appearing tissue
El-Abtah, 2022 ⁶	ml/c-Cr	Shorter-term survivors (OS < 9 months) exhibited decreased ml/c-Cr in both the intratumoral and contralateral normal appearing tissues. Levels of ml/c-Cr in the normal appearing tissue was predictive of survivorship at 1 day, 4 weeks, and 8 weeks after AAT initiation

AAT, anti-angiogenic therapy; PCho/GPC, ratio of phosphocholine to glycerophosphocholine; NAA, N-acetylaspartate; tCho/NAA, ratio of total choline to NAA; NAA/Cho, ratio of NAA to choline; Cho/NAA, ratio of choline to NAA; NAA/c-Cr, ratio of NAA to creatine in the contralateral normal appearing tissue; Cho/c-Cr, ratio of choline to creatine in the contralateral normal appearing tissue; NAA/cr, ratio of NAA to creatine; Cho/cr, ratio of choline to creatine; OS, overall survivorship; tCho/c-Cr, ratio of total choline to creatine in contralateral normal appearing white matter tissue; Lac, lactate; GBM, glioblastoma; RT, radiotherapy; ml, myo-inositol; ml/c-Cr, ml normalized to creatine in the contralateral normal appearing tissue.

note, the post-treatment scans and MRSI acquisition were performed at a timepoint between 3 and 5 weeks after AAT initiation.²⁵

Kim et al.³⁰ analyzed levels of NAA/Cho, NAA normalized to creatine in the contralateral normal appearing tissue (NAA/c-Cr), and Cho normalized to Cr in the contralateral normal appearing tissue (Cho/c-Cr) before cedarinib initiation, and multiple timepoints afterwards. Intratumoral NAA/Cho was significantly increased through day 56, which was driven by an increase in intratumoral NAA/c-Cr and a decrease in Cho/c-Cr. Intriguingly, at the 56-day timepoint, elevated intratumoral NAA/Cho was predictive of 6 month OS. A similar finding was reported by Ratai et al. and Talati et al., where increases in intratumoral and peritumoral NAA/Cho relative to pretreatment levels were predictive of progression free survival at 6 months (PFS-6) and OS at 9 months, respectively.^{12,27} Ratai et al. reported that increased tumoral NAA/Cho at 8 weeks was associated with PFS-6 and a decreased peritumoral Cho/Cr and increased NAA/Cr and NAA/Cho at 16 weeks after AAT were predictive of PFS-6 and OS at 1-year.²⁷ Further, Talati et al.¹² showed that increased intratumoral NAA/Cho relative to pretreatment baseline was predictive of OS at 1-day, 2-weeks, 8-weeks, and 16-weeks, with survival analyses revealing that those with NAA/Cho greater than an optimized cutoff had a significantly higher median OS compared to those with decreased NAA/Cho (275 days versus 175 days).

The association between survivorship and markers of cellular proliferation were also reported by Andronesi et al.³¹ for 21 patients with GBM treated with cedarinib and chemoradiation. Survivors were dichotomized according to the cohort's median survivorship of 18.2 months, and longer-term survivors (OS > 18.2 months) had significant reductions in levels of total choline normalized to creatine in the contralateral normal appearing tissue (tCho/c-Cr) at 15 and 29 days after initiation of combination therapy.³¹ Interestingly, when compared to other MR imaging markers such as relative cerebral blood flow and contrast-enhanced T1 volume, tCho/c-Cr was the most robust at predicting OS after 1-month of treatment based on receiver operating characteristics analyses.³¹

Stadlbauer et al.²² analyzed metabolic markers from 18 patients who were treated with AAT. Of the 8 patients who showed evidence of response to treatment based on retrospective MRI analyses, there was a significant decrease in Cho and Cho/NAA and a significant increase in NAA/Cr and NAA within the lesion between the time of first examination (pre-AAT initiation), and the third examination (234 days post-AAT initiation). The 10 patients who showed evidence of pseudo response displayed opposite trends, with significant decreases in NAA and NAA/Cr and significant increases in Cho/NAA within the lesion between the first and third examinations.²² Notably, 75% of patients who responded to AAT, also displayed remote GBM progression.²²

Hattingen et al.¹⁷ reported results on the PCho/GPC ratio, a marker of tumor proliferation, which is readily detectable by ³¹P MRSI. Patients in the short overall survivorship (OS) group (< median OS) had elevated intratumoral PCho/GPC relative to the contralateral normal appearing tissue prior to AAT initiation. Eight weeks after AAT initiation, there was a significant decrease in PCho/GPC in both those with

short and long OS, followed by a significant increase at the time of progression.¹⁷ The authors conclude that elevated PCho/GPC was a negative predictor of AAT response.¹⁷

MR Spectroscopic Markers of Hypoxia and Enhanced Glycolysis

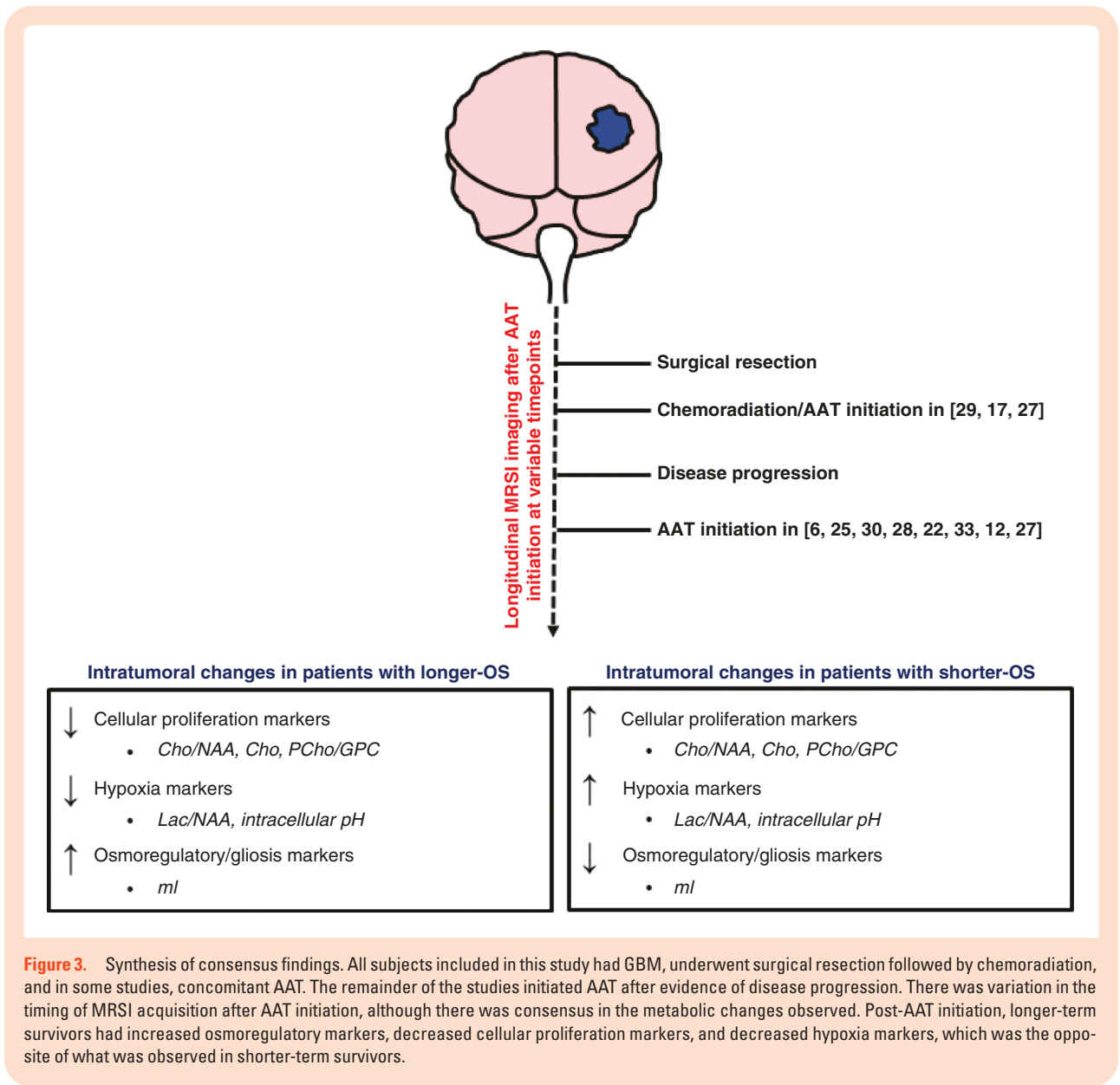
Four studies (4/11; 36.4%) discussed the metabolic changes associated with tumor hypoxia and necrosis in relation to AAT^{12,25,26,29} (Table 3). Talati et al.¹² reported that intratumoral changes in Lac/NAA relative to the baseline timepoint predicted survivorship of patients with rGBM treated with AAT. Ninety percent of their cohort with elevated Lac/NAA from baseline (prior to AAT initiation) had an OS less than 9 months. Additionally, receiver operating characteristic curves revealed that Lac/NAA was predictive of overall survivorship at 1-day, 2-weeks, 4-weeks, 8-weeks, and 16-weeks post-AAT initiation, with higher levels of Lac/NAA predictive of shorter survivorship.¹²

Nelson et al.²⁶ tracked metabolic changes in Lac and lipids, markers of hypoxia and necrosis, across 4 timepoints: baseline (pre-AAT initiation), between 1 and 3 weeks after AAT initiation, 4 weeks after AAT initiation, and approximately 4 months after AAT initiation. They reported that lactate and lipids relative to NAA in the contralateral normal appearing tissue decreased at all timepoints relative to baseline, which was significant at 4-weeks and 4-months after AAT initiation.²⁶ Similarly, Jeon et al. reported data on Lac from a single GBM voxel located in the splenium of the corpus callosum before and after intra-arterial cerebral infusion of AAT. They reported a robust Lac peak before therapy, which showed evidence of modest decrease after therapy, although no statistical analyses were performed to confirm significance since it was not the primary outcome measure of interest.²⁵

Wenger et al.²⁹ reported results from 14 patients with recurrent GBM, classified based on Response Assessment in Neuro-Oncology (RANO). Prior to initiation of AAT, the intracellular pH in the region of radiographically unaffected, but subsequent tumor, was significantly elevated (pH = 7.065) compared to normal appearing tissue on the contralateral hemisphere to the tumor (pH = 7.017). The intracellular pH of the subsequent tumor region decreased to 7.044 at the time of best response to AAT (based on RANO criteria), followed by a significant increase to a pH of 7.085 at the time of disease progression.²⁹ This is consistent with the author's finding that elevated intracellular pH in unaffected tissue was predictive of disease progression in patients with rGBM treated with AAT.

MR Spectroscopic Markers of Gliosis and Osmotic Dysregulation

Two studies (2/11; 18.2%) discussed the metabolic changes associated with osmotic dysregulation after initiation of AAT^{28,6} (Table 3). Steidl et al.²⁸ reported results from 30 patients with rGBM (based on RANO criteria) treated with AAT. ml was significantly increased in the intratumoral and contralateral normal appearing tissue after AAT compared to baseline. Notably, the authors reported that this effect was more pronounced in the intratumoral tissue,



which showed a 93.8% increase in ml post-treatment.²⁸ Survivorship analyses revealed that there were significant group differences in ml between longer- and shorter-term survivors in the contralateral normal appearing tissue, but not in the intratumoral tissue.²⁸ Specifically, longer-term survivors had elevated ml levels in the contralateral normal appearing tissue and a greater difference in ml levels between both volumes compared to shorter-term survivors.²⁸

El-Abtah et al.⁶ reported results from the same marker, ml, with the exception that it was normalized to creatine within the contralateral normal appearing tissue (ml/c-Cr). Levels of ml/c-Cr within the intratumoral and contralateral normal appearing tissue were significantly lower at baseline (prior to AAT initiation) in those who had an OS lower than 9 months. Additionally, decreased ml/c-Cr in the intratumoral tissue was predictive of shorter-term survivorship at 1-day and 8-weeks post-AAT initiation.⁶

Survivorship analyses revealed that those with an elevated ml/c-Cr had a greater mean OS compared to those with decreased levels ml/c-Cr.⁶ A similar effect was observed in the contralateral normal appearing tissue, where lower ml/c-Cr levels were predictive of shorter-term survivorship (OS < 9 months) at 1-day, 4-weeks, and 8-weeks after AAT initiation.⁶

Synthesis of Consensus Findings

Key consensus findings from all 11 studies are illustrated in Figure 3. All patients in the included studies had evidence of GBM and underwent surgical resection followed by treatment regimens that included chemoradiation and either AAT combination therapy or monotherapy. However, there was variability regarding when AAT was initiated, with some studies initiating AAT concomitantly with chemoradiation and others only after documented

recurrence. Importantly, there was heterogeneity regarding the timing of longitudinal MRSI, with some studies assessing metabolic changes as early as 1-day after AAT initiation and others up to 6–9 months afterwards (Figure 3). Despite differences in timing of MRSI acquisition, there were general trends in metabolic marker changes between longer- and shorter-term survivors. Longer-term survivors had evidence of increased osmoregulator markers, decreased cellular proliferation markers, and decreased hypoxia markers post-AAT initiation, which was the opposite of what was observed for shorter-term survivors (Figure 3).

Discussion

To the best of our knowledge, this represents the first systematic review addressing metabolic changes detected by single or multi-voxel MRS after initiation of AAT. All studies utilized MRSI, and there is evidence that MRSI can offer clinically valuable information to the neurooncologists and neuroradiologists regarding the course of GBM progression after AAT initiation. Despite there being few studies, a common theme was that current MRS markers can be categorized into those of proliferation, hypoxia/necrosis, osmoregulation, all of which are actively fluctuating throughout the course of GBM and treatment with AAT. Although there was heterogeneity in MRSI acquisition parameters, there was consistency in the main findings.

From our review of the literature, the most common reported marker involving AAT's anti-proliferative effects were Cho and NAA, where a decreased ratio of Cho/NAA is consistent with a better prognosis and longer-term survivorship. This is likely due to decreased membrane synthesis and degradation, which involves choline-containing phospholipids that are involved in signal transduction.^{9,34} Histopathological analyses have also revealed that Cho is a robust proxy for glioma cell density, and thus can be useful in distinguishing between actively proliferating neoplastic lesions and those with acellular necrosis.³⁵ The elevated intratumoral Cho/NAA ratios observed in shorter-term survivors are likely due to a coupling between elevated Cho and decreased NAA and suggest failure of AAT.^{12,22,25,27} Specifically, decreases in NAA can be seen as a replacement of viable neural tissue and compromised integrity of axonal structure.³⁶

Interestingly, Kim et al. and Hattingen et al. reported fluctuations in markers of proliferation after AAT in their cohorts. Specifically, during the early stages of AAT, there was a marked decrease in PCho/GPC and Cho/c-Cr, which was reversed at the time of disease progression.^{17,30} This phenomenon is consistent with an initial normalization of the abnormal microvasculature feeding the tumor, resulting in enhanced oxygenation, reduced vasogenic edema, and increased sensitization to RT and cytotoxic agents.³⁷ However, treatment resistance followed by tumor progression in GBM is inevitable, which was detected by MRSI in the aforementioned studies at the time of progression.³⁷ An animal study by Kamoun et al.³⁸ showed that treatment with the VEGF-targeted kinase inhibitor, cediranib, resulted in decreased vasogenic edema without changes to tumor proliferation and apoptotic activity. Ergo,^{17,30} although AAT

may improve symptoms such as edema and reduce the need for continued steroid therapy in patients, there is evidence for GBMs developing resistance to therapy, which may correlate with the elevated Cho/NAA and PCho/GPC at the time of progression.

Elevated levels of Lac and lipids are accepted markers of necrosis and hypoxia and may mark the transition of GBM from an infiltrative phenotype to a more malignant one.^{11,39} It is thought that anaerobic respiration due to proliferative activity and hypoxia results in the production of Lac and an acidic microenvironment, which results in the accumulation of protons within the intracellular compartments of the glial cells.^{40,41} This is consistent with the findings reported by Hattingen et al.,^{29,42} as the accumulation of intracellular protons trigger the upregulation of specialized pumps that remove the excess protons into the extracellular environment, resulting in a coupling between elevated intracellular pH and active tumor proliferation and hypoxia.

The Lac findings by Jeon et al. and Nelson et al. are most consistent with a model of vascular normalization, whereby the tumor receives increased perfusion and oxygenation early in the course of AAT, which is correlated with improved survivorship.^{26,43,44} However, those studies do not contain sufficient longitudinal follow-up to determine whether those tumors ultimately progressed to a model of vascular pruning whereby the vascular network supplying the tumor is trimmed, resulting in hypoxia, decreased effectiveness of therapeutics, and increased metastasis.⁴⁵ Indeed, the study by Talati et al.¹² is suggestive of vascular pruning, whereby the elevated Lac/NAA was predictive of shorter-term OS. These findings are further supported by animal studies which have shown that GBM adapts to AAT by undergoing extensive metabolic re-programming. Fack et al.⁴⁶ reported results from ¹³C₆-glucose metabolic flux analysis by single voxel ¹³C MRS which showed that subsequent to AAT, there was an increased flux of ¹³C₆-glucose, increased Lac, and decreased levels of metabolites associated with the Krebs cycle. These results were confirmed by MRSI and immunohistochemical analyses which showed a marked upregulation of lactate dehydrogenase in tumors, potentially explaining the increased tumor invasion observed after AAT.⁴⁶

The findings by El-Abtah et al. and Steidl et al. both suggested that osmotic dysregulation may be a hallmark of GBM, and that the short TE MRS metabolite, ml, can predict survivorship as early as before AAT initiation. Interestingly, both studies reported changes in ml within the contralateral, radiographically normal, appearing tissue.^{6,28} These results can be partly explained by tumor invasion that extends to the contralateral hemisphere, which has been confirmed by autopsy and animal studies.^{47,48} Additionally, increased vasogenic edema, which is a marker of pseudoresponse to AAT, is characteristic of invasive tumors and may result in extensive damage to the BBB.^{22,49,50} Therefore, the decreased intratumoral ml observed in shorter-term survivors may be suggestive of AAT failure, damaged BBB, and a decreased ability for osmoregulation.^{6,28} An important consideration when measuring levels of ml is that its resonance overlaps with that of Gly at short TE, making the distinction between both markers difficult. Nonetheless, this issue can be circumvented by using 7T scanners, as previous work has demonstrated that using

a higher strength magnetic field with single spin-echo excitation schemes can decouple the ml from the Gly signal, resulting in the reliable quantification of the ml signal.⁵¹ However, 7T scanners are not readily available for routine clinical scans across hospital systems, and therefore, this option may be limited.

Most of the studies incorporated multi-voxel intermediate TE MRSI, which detected the majority of metabolic ratios related to cellular proliferation such as Cho/NAA and Cho/c-Cr, in addition to markers of hypoxia such as Lac/NAA. However, there is value in acquiring short TE metabolites, such as ml, because it can relay valuable information pertaining to the disruption of the BBB and response to AAT. Furthermore, short TE can detect all of the markers of cellular proliferation and hypoxia reported in our results to help assess response to AAT. Consequently, we recommend acquisition of short TE, multi-voxel, MRS data whenever possible to allow for a more comprehensive assessment of the heterogenous tumor microenvironment associated with GBMs. However, if lactate is of particular importance to the clinical team, then intermediate TE should be considered as this marker is preferentially detected at intermediate TE to better distinguish it from the overlapping lipid signal.⁵² While higher magnetic field strengths result in better signal-to-noise ratio and spectral resolution, 1.5T and 3T acquisition are sufficient to quantify the reported metabolic markers that can prognosticate outcomes following AAT.

Based on the results of this review, a scan prior to initiation of AAT is necessary to establish what the baseline tumor microenvironment shows. For instance, the study by Talati et al. and Ratai et al. reported that changes in NAA/Cho and Lac/NAA relative to baseline were predictive of outcome rather than the absolute metabolic ratios at a given time point.¹² The timing of MRS acquisition was highly variable throughout the included studies, underscoring the lack of a consensus protocol regarding the optimal time to acquire MRS data. Nonetheless, the study by El-Abtah et al.⁶ suggests that levels of ml as early as 1-day post-AAT initiation can be robust predictors of patient survivorship, which can help identify those who will likely fail AAT and thus are suitable candidates for salvage therapies. Overall, a baseline scan prior to AAT initiation is essential and there still remains a need to standardize the timing of MRS acquisition after AAT initiation.

Limitations

Our study had some limitations, which are common to systematic literature reviews of this kind. First, there were few studies that met inclusion criteria, limiting our ability to perform a meta-analysis. Second, due to the possibility of a publication bias, there may have been a disproportionate number of studies with positive findings, which limits our ability to assess the true value of MR spectroscopic markers in predicting survival. Third, there could have been a selection bias regarding which studies were deemed to have met the inclusion and exclusion criteria, although we utilized a blinded review process to minimize this possibility. Fourth, the criteria used for

ensuring quality control of the spectra varied across the studies. This is an important consideration given that certain brain regions such as the temporal lobe are more prone to susceptibility artifact. Fifth, there was variation regarding the timing of longitudinal MRSI after initiation of AAT, with all studies using different timepoints to assess metabolic changes. Therefore, despite there being a general consensus regarding metabolic changes post-AAT initiation in longer- and shorter-term survivors, there is a need to validate these markers at similar timepoints using a standardized protocol prior to routine clinical integration. Future work should focus on standardizing the timing of scans post-AAT initiation, as well as validating the spectroscopic markers such that they can be routinely incorporated in multi-center clinical trials and clinical use.⁵³

Overall, there is utility in incorporating MRSI alongside clinical follow-up scans to track changes in GBM metabolism in response to AAT.

Conclusions

MRSI can detect changes in cellular proliferation, hypoxia/necrosis, and osmoregulation in response to AAT and can be integrated with other forms of advanced MR imaging to help inform neurooncologists regarding metabolic changes in GBMs after AAT initiation.

Keywords

anti-angiogenic therapy | bevacizumab | glioblastoma | MR spectroscopy | GBM | MRSI

Funding

This study was supported by Grant R01 CA190901 from the National Institutes of Health (NIH) to E.M.R.

Conflict of Interest. E.M.R. is an advisory board member for BrainSpec and J.D. has received royalties from Wolters Kluwer as an author for UpToDate and consulting fees from Blue Earth Diagnostics and Unum Therapeutics.

Authorship Statement. M.E.E., P.T., and E.M.R. were involved in the design and conception of this manuscript. M.E.E. and E.M.R. performed the literature search. M.E.E. compiled the primary manuscript. M.E.E. compiled the figures. E.M.R., P.T., J.D., E.R.G., and E.M.R. critically revised the manuscript. All authors have approved the manuscript as it is written.

References

- Tan AC, Ashley DM, López GY, et al. Management of glioblastoma: state of the art and future directions. *CA Cancer J Clin.* 2020;70(4):299–312.
- Arevalo OD, Soto C, Rabiei P, et al. Assessment of glioblastoma response in the era of bevacizumab: longstanding and emergent challenges in the imaging evaluation of pseudoresponse. *Front Neurol.* 2019;10:460.
- Gilbert MR, Dignam JJ, Armstrong TS, et al. A randomized trial of bevacizumab for newly diagnosed glioblastoma. *N Engl J Med.* 2014;370(8):699–708.
- Chinot OL, Wick W, Mason W, et al. Bevacizumab plus radiotherapy-temozolomide for newly diagnosed glioblastoma. *N Engl J Med.* 2014;370(8):709–722.
- Falchetti ML, D'Alessandris QG, Pacioni S, et al. Glioblastoma endothelium drives bevacizumab-induced infiltrative growth via modulation of PLXDC1. *Int J Cancer.* 2019;144(6):1331–1344.
- El-Abtah ME, Wenke MR, Talati P, et al. Myo-inositol levels measured with MR spectroscopy can help predict failure of antiangiogenic treatment in recurrent glioblastoma. *Radiology.* 2022;302(2):410–418.
- Moffett JR, Ross B, Arun P, Madhavarao CN, Nambodiri AMA. N-Acetylaspartate in the CNS: from neurodiagnostics to neurobiology. *Prog Neurobiol.* 2007;81(2):89–131.
- Yerli H, Ağildere AM, Ozen O, et al. Evaluation of cerebral glioma grade by using normal side creatine as an internal reference in multi-voxel 1H-MR spectroscopy. *Diagn Interv Radiol.* 2007;13(1):3–9.
- Horská A, Barker PB. Imaging of brain tumors: MR spectroscopy and metabolic imaging. *Neuroimaging Clin N Am.* 2010;20(3):293–310.
- de la Cruz-López KG, Castro-Muñoz LJ, Reyes-Hernández DO, García-Carrancá A, Manzo-Merino J. Lactate in the regulation of tumor microenvironment and therapeutic approaches. *Front Oncol.* 2019;9:1143.
- Oz G, Alger JR, Barker PB, et al. Clinical proton MR spectroscopy in central nervous system disorders. *Radiology.* 2014;270(3):658–679.
- Talati P, El-Abtah M, Kim D, et al. MR spectroscopic imaging predicts early response to anti-angiogenic therapy in recurrent glioblastoma. *Neurooncol Adv.* 2021;3(1):vdab060.
- Hattingen E, Raab P, Franz K, et al. Myo-inositol: a marker of reactive astrogliosis in glial tumors? *NMR Biomed.* 2008;21(3):233–241.
- Hattingen E, Lanfermann H, Quick J, Franz K, Zanella FE, Pilatus U. 1H MR spectroscopic imaging with short and long echo time to discriminate glycine in glial tumours. *MAGMA.* 2009;22(1):33–41.
- Menendez JA, Lupu R. Fatty acid synthase and the lipogenic phenotype in cancer pathogenesis. *Nat Rev Cancer.* 2007;7(10):763–777.
- Themes UFO. MR spectroscopy and the biochemical basis of neurologic disease. *Radiology Key.* Published November 8, 2018. <https://radiologykey.com/mr-spectroscopy-and-the-biochemical-basis-of-neurologic-disease/>. Accessed March 10, 2022.
- Hattingen E, Bähr O, Rieger J, et al. Phospholipid metabolites in recurrent glioblastoma: in vivo markers detect different tumor phenotypes before and under antiangiogenic therapy. *PLoS One.* 2013;8(3):e56439.
- Ha DH, Choi S, Oh JY, et al. Application of 31P MR spectroscopy to the brain tumors. *Korean J Radiol.* 2013;14(3):477–486.
- Negendank W. Studies of human tumors by MRS: a review. *NMR Biomed.* 1992;5(5):303–324.
- Wilson M, Andronesi O, Barker PB, et al. Methodological consensus on clinical proton MRS of the brain: review and recommendations. *Magn Reson Med.* 2019;82(2):527–550.
- Zhu H, Barker PB. MR spectroscopy and spectroscopic imaging of the brain. *Methods Mol Biol.* 2011;711:203–226.
- Stadlbauer A, Pichler P, Karl M, et al. Quantification of serial changes in cerebral blood volume and metabolism in patients with recurrent glioblastoma undergoing antiangiogenic therapy. *Eur J Radiol.* 2015;84(6):1128–1136.
- Liberati A, Altman DG, Tetzlaff J, et al. The PRISMA statement for reporting systematic reviews and meta-analyses of studies that evaluate health care interventions: explanation and elaboration. *Ann Intern Med.* 2009;151(4):W65–W94.
- Vaughn MG, Howard MO. Adolescent substance abuse treatment: a synthesis of controlled evaluations. *Res Soc Work Pract.* 2004;14(5):325–335.
- Jeon JY, Kovanlikaya I, Boockvar JA, et al. Metabolic response of glioblastoma to superselective intra-arterial cerebral infusion of bevacizumab: a proton MR spectroscopic imaging study. *Am J Neuroradiol.* 2012;33(11):2095–2102.
- Nelson SJ, Li Y, Lupo JM, et al. Serial analysis of 3D H-1 MRSI for patients with newly diagnosed GBM treated with combination therapy that includes bevacizumab. *J Neurooncol.* 2016;130(1):171–179.
- Ratai EM, Zhang Z, Snyder BS, et al. Magnetic resonance spectroscopy as an early indicator of response to anti-angiogenic therapy in patients with recurrent glioblastoma: RTOG 0625/ACRIN 6677. *Neuro Oncol.* 2013;15(7):936–944.
- Steidl E, Pilatus U, Hattingen E, et al. Myoinositol as a biomarker in recurrent glioblastoma treated with bevacizumab: a 1H-magnetic resonance spectroscopy study. *PLoS One.* 2016;11(12):e0168113.
- Wenger KJ, Hattingen E, Franz K, et al. Intracellular pH measured by 31 P-MR-spectroscopy might predict site of progression in recurrent glioblastoma under antiangiogenic therapy. *J Magn Reson Imaging.* 2017;46(4):1200–1208.
- Kim H, Catana C, Ratai EM, et al. Serial magnetic resonance spectroscopy reveals a direct metabolic effect of cediranib in glioblastoma. *Cancer Res.* 2011;71(11):3745–3752.
- Andronesi OC, Esmaeili M, Borra RJH, et al. Early changes in glioblastoma metabolism measured by MR spectroscopic imaging during combination of anti-angiogenic cediranib and chemoradiation therapy are associated with survival. *NPJ Precis Oncol.* 2017;1:20.
- Duyn JH, Gillen J, Sobering G, van Zijl PC, Moonen CT. Multisection proton MR spectroscopic imaging of the brain. *Radiology.* 1993;188(1):277–282.
- Kreis R. Issues of spectral quality in clinical 1H-magnetic resonance spectroscopy and a gallery of artifacts. *NMR Biomed.* 2004;17(6):361–381.
- Tayebati SK, Amenta F. Choline-containing phospholipids: relevance to brain functional pathways. *Clin Chem Lab Med.* 2013;51(3):513–521.
- Gupta RK, Cloughesy TF, Sinha U, et al. Relationships between choline magnetic resonance spectroscopy, apparent diffusion coefficient and quantitative histopathology in human glioma. *J Neurooncol.* 2000;50(3):215–226.
- Sibtain NA, Howe FA, Saunders DE. The clinical value of proton magnetic resonance spectroscopy in adult brain tumours. *Clin Radiol.* 2007;62(2):109–119.
- Batchelor TT, Reardon DA, de Groot JF, Wick W, Weller M. Antiangiogenic therapy for glioblastoma: current status and future prospects. *Clin Cancer Res.* 2014;20(22):5612–5619.
- Kamoun WS, Ley CD, Farrar CT, et al. Edema control by cediranib, a vascular endothelial growth factor receptor-targeted kinase inhibitor, prolongs survival despite persistent brain tumor growth in mice. *J Clin Oncol.* 2009;27(15):2542–2552.
- Thorsen F, Jirak D, Wang J, et al. Two distinct tumor phenotypes isolated from glioblastomas show different MRS characteristics. *NMR Biomed.* 2008;21(8):830–838.
- Owen CS. Dependence of proton generation on aerobic or anaerobic metabolism and implications for tumour pH. *Int J Hyperth.* 1996;12(4):495–499.
- Rao JU, Coman D, Walsh JJ, et al. Temozolomide arrests glioma growth and normalizes intratumoral extracellular pH. *Sci Rep.* 2017;7(1):7865.

42. Lagadic-Gossmann D, Huc L, Lecureur V. Alterations of intracellular pH homeostasis in apoptosis: origins and roles. *Cell Death Differ.* 2004;11(9):953–961.
43. Jain RK. Antiangiogenesis strategies revisited: from starving tumors to alleviating hypoxia. *Cancer Cell.* 2014;26(5):605–622.
44. Gerstner ER, Emblem KE, Yen YF, et al. Vascular dysfunction promotes regional hypoxia after bevacizumab therapy in recurrent glioblastoma patients. *Neurooncol Adv* 2020;2(1):vdaa157.
45. Jain RK. Normalizing tumor microenvironment to treat cancer: bench to bedside to biomarkers. *J Clin Oncol.* 2013;31(17):2205–2218.
46. Fack F, Espedal H, Keunen O, et al. Bevacizumab treatment induces metabolic adaptation toward anaerobic metabolism in glioblastomas. *Acta Neuropathol.* 2015;129(1):115–131.
47. Nagashima G, Suzuki R, Hokaku H, et al. Graphic analysis of microscopic tumor cell infiltration, proliferative potential, and vascular endothelial growth factor expression in an autopsy brain with glioblastoma. *Surg Neurol.* 1999;51(3):292–299.
48. Crommentuijn MHW, Schetters STT, Dusoswa SA, et al. Immune involvement of the contralateral hemisphere in a glioblastoma mouse model. *J ImmunoTher Cancer.* 2020;8(1):e000323.
49. Dubois LG, Campanati L, Righy C, et al. Gliomas and the vascular fragility of the blood brain barrier. *Front Cell Neurosci.* 2014;8:418.
50. Artzi M, Liberman G, Blumenthal DT, Aizenstein O, Bokstein F, Ben Bashat D. Differentiation between vasogenic edema and infiltrative tumor in patients with high-grade gliomas using texture patch-based analysis. *J Magn Reson Imaging.* 2018.
51. Gambarota G, Meke R, Xin L, et al. In vivo measurement of glycine with short echo-time 1H MRS in human brain at 7 T. *MAGMA.* 2009;22(1):1–4.
52. Lange T, Dydak U, Roberts TPL, et al. Pitfalls in lactate measurements at 3T. *Am J Neuroradiol.* 2006;27(4):895–901.
53. Deelchand DK, Berrington A, Noeske R, et al. Across-vendor standardization of semi-LASER for single-voxel MRS at 3T. *NMR Biomed.* 2021;34(5):e4218.